Radiotherapy and Oncology 139 (2019) 28–33

Contents lists available at ScienceDirect

Radiotherapy and Oncology

journal homepage: www.thegreenjournal.com

Original Article

PHASER: A platform for clinical translation of FLASH cancer radiotherapy

Peter G. Maxim [a,**], Sami G. Tantawi [b,**], Billy W. Loo Jr. [c,d,*]

[a] Department of Radiation Oncology, Indiana University School of Medicine; [b] SLAC National Accelerator Laboratory; [c] Department of Radiation Oncology; and [d] Stanford Cancer Institute, Stanford University School of Medicine, United States

ARTICLE INFO

Article history:
Received 27 December 2018
Received in revised form 25 April 2019
Accepted 3 May 2019
Available online 6 June 2019

Keywords:
PHASER
FLASH
Ultra-rapid radiation therapy
Very high-energy electron radiotherapy

ABSTRACT

Pluridirectional high-energy agile scanning electronic radiotherapy (PHASER) is next-generation medical linac technology for ultra-rapid highly conformal image-guided radiation, fast enough to "freeze" physiological motion, affording improved accuracy, precision, and potentially superior FLASH radiobiological therapeutic index. Designed for compactness, economy, and clinical efficiency, it is also intended to address barriers to global access to curative radiotherapy.

Cancer is a leading and epidemically increasing cause of death globally in both the developed and developing world. Because radiation therapy is a pillar of curative cancer therapy, two major challenges must be addressed to reduce cancer mortality substantially: (1) fundamentally increasing the therapeutic index of radiotherapy, maximizing tumor eradication while minimizing toxicity; (2) increasing global access to the highest quality radiotherapy.

The main technical advances increasing radiotherapy therapeutic index in the past two decades have been maximizing the dose differential between tumors and normal tissues through dose conformity (*e.g.*, intensity-modulated radiation therapy [IMRT], hadron therapy) and reduction of uncertainties and thus target volumes, mainly by image-guidance for more accurate target delineation and localization. A major remaining hurdle to ultimate precision is motion of the patient and tumor during radiotherapy. Conventional "motion management" approaches all assume that radiotherapy delivery is much slower than physiologic motion.

Recent preclinical observations of dramatically reduced normal tissue toxicity and preserved anti-tumor efficacy with ultra-rapid FLASH radiotherapy (dose rates exceeding ~50 Gy/second), reported in this special issue of *Radiotherapy and Oncology* and inspired by the work of Favaudon et al. [6], suggest a fundamentally new approach to increasing the therapeutic index of radiotherapy. Clinical translation of ultra-rapid image-guided radiotherapy promises to provide a more fundamental motion management strategy, effectively "freezing" physiologic motion, while exploiting new FLASH radiobiological advantages.

To realize this goal of ultra-rapid image-guided radiotherapy delivery in a compact and economical platform, we are developing Pluridirectional High-energy Agile Scanning Electronic Radiotherapy (PHASER), comprising several innovations in accelerator and radiofrequency science and medical physics. Here we provide an overview of the technologies underlying PHASER.

Core technologies of PHASER

Existing clinical technologies are orders of magnitude too slow to deliver FLASH to typical deep-seated radiotherapy targets of clinically relevant volume. The highest dose rate produced by current photon systems in flattening filter-free mode at 10 MV energy is ~10 Gy/min for IMRT plans. An increase of at least 300-fold is needed to achieve dose rates exceeding 50 Gy/s. Recently, clinical electron and proton therapy machines have been configured to produce dose rates >50 Gy/sec in a small volume from a single beam direction, enabling preclinical small animal FLASH radiobiology research with these systems, but still far from enabling FLASH radiotherapy of typical clinical targets in humans [23,19,13]. Similarly, highly conformal doses are currently produced through multiple beam directions and intensity-modulation of each beam using mechanical systems (gantry and multi-leaf collimator [MLC]) that are incompatible with sub-second delivery. Ultra-rapid delivery must also be integrated with rapid, simultaneous, high-quality

* Corresponding author at: Department of Radiation Oncology & Stanford Cancer Institute, Stanford University School of Medicine, 875 Blake Wilbur Drive, Stanford, CA 94305, United States.

** Co-corresponding authors at: Department of Radiation Oncology, Indiana University School of Medicine, 535 Barnhill Drive, Indianapolis, IN 46202, United States (P.G. Maxim); SLAC National Accelerator Laboratory, 2575 Sand Hill Road, Menlo Park, CA 94025, United States (S.G. Tantawi).

E-mail addresses: PMaxim@iu.edu (P.G. Maxim), Tantawi@slac.stanford.edu (S.G. Tantawi), BWLoo@Stanford.edu (B.W. Loo Jr.).

https://doi.org/10.1016/j.radonc.2019.05.005
0167-8140/

volumetric imaging of the treatment volume. For clinical practicality, the overall form factor and power requirements should fit within existing standard vaults and infrastructure.

Thus the core technical innovations of PHASER comprise: (1) highly compact, economical, and power-efficient linear accelerator and radiofrequency (RF) power sources based on fundamentally new accelerator science, producing hundreds of times the beam output of conventional medical linacs; (2) a rapid RF power distribution system supplying an array of 16 stationary beamlines providing a full complement of non-coplanar (conical geometry) beams for highly conformal radiotherapy, eliminating mechanical gantry rotation; (3) rapid electronically scanned highly intensity-modulated photon beams from scanning an electron beam on a stationary target and collimator array, eliminating mechanical collimator motion; (4) integration of full ring diagnostic quality/speed multi-detector CT, sharing a common isocenter with the non-coplanar treatment beamlines.

Accelerator structure (DRAGON)

Producing very high accelerating gradients (>100 MeV/meter) in linear accelerators is limited by RF breakdown (arcing) on the surface of the accelerating structure. The major discovery from recent research on this complex phenomenon pertains to the role of surface magnetic fields [9,5,12]. High surface magnetic fields produce localized pulsed heating, causing surface artifacts that lead to RF breakdown. These discoveries have led to a completely new paradigm in accelerator design: optimizing accelerating cell geometry for minimal peak surface magnetic fields not only reduces RF breakdown at high gradients, but greatly improves power efficiency by minimizing losses to waste heating of the structure, *i.e.*, high shunt impedance.

In our new design for electron linacs, Distributed RF-coupling Architecture with Genetically Optimized cell desigN (DRAGON), the shape of the accelerating cells is derived from genetic optimization to minimize the peak surface magnetic fields [28] (Fig. 1A). Distributing the RF power to each cell independently without coupling between cells provides much greater degrees of freedom for the cell optimization. The phase advance between cells is then controlled by the phased advance of the RF in the distribution manifold that feeds RF power to each cell individually. Because the manifold is a broadband non-resonance structure, precise phase advance per cell can be achieved even at high frequencies (including up to X- and Ku-bands) with low sensitivity to manufacturing tolerances [28].

The shunt impedances of DRAGON accelerator structures to date varies with the frequency band, ranging from approximately 130 MΩ/m at S-band to 200 MΩ/m at X-band, a factor of about 2.5–4 times that of conventional medical linacs (a more detailed discussion is provided in the Appendix). For the anticipated operating parameters of PHASER (including beam energy and current), this translates to an efficiency (proportion of applied RF power transferred to the electron beam) of about 80%, compared to typically about 20% (ranging from 18 to 45%) in conventional medical linacs depending on the frequency band. Therefore, the duty factor can be much higher than that of conventional linacs because the majority of the applied RF power is transferred to the electron beam rather than heating the structure.

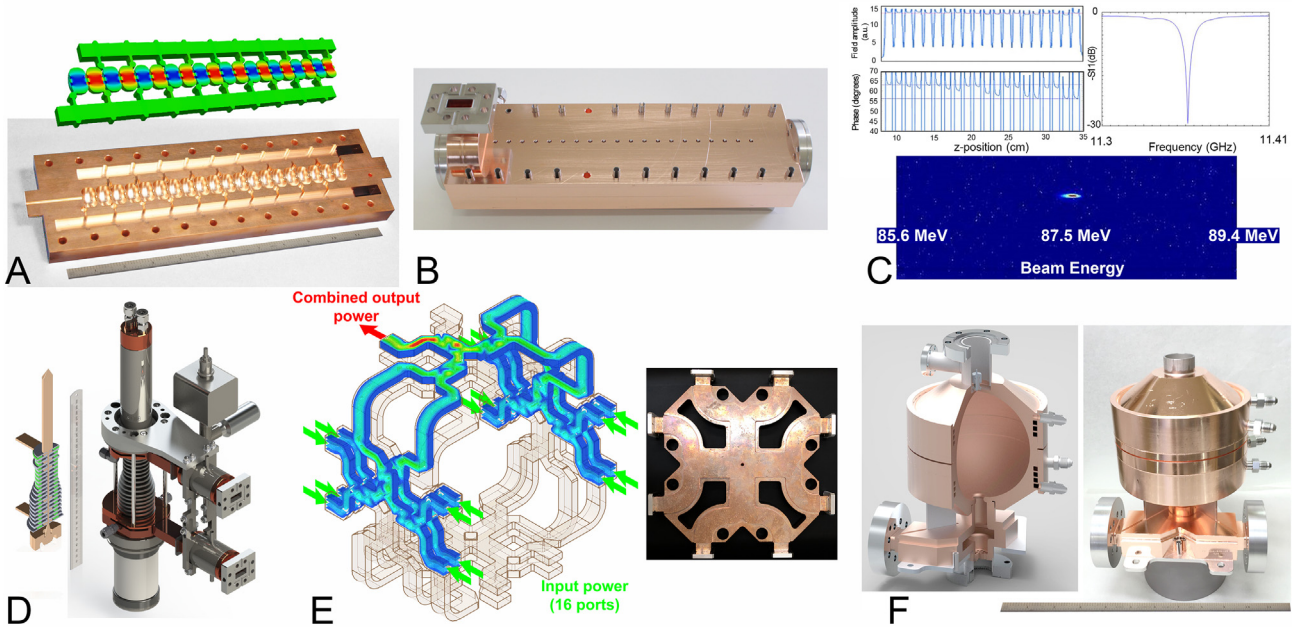

Fig. 1. (A) Twenty-cell prototype of Distributed RF-coupling Architecture with Genetically Optimized cell desigN (DRAGON) linear accelerator structure. RF power is fed individually to each cell with specified phase advance via an RF distribution manifold (the feeding waveguides to the sides of the cells on the center axis). The cell shape is optimized to minimize peak surface magnetic fields for maximum power efficiency and resistance to RF breakdown (top). Half of the structure produced by 3-D machining integrating the optimized cells, RF distribution manifold, and other supporting features such as water cooling channels in a monolithic part (bottom) rather than the conventional cell by cell construction. (Ruler = 30.5 cm). (B) Assembled structure with the two halves brazed together. (C) Cold testing demonstrating uniform field amplitude and phase across the cells and a single resonance frequency for the entire structure rather than the typical 20 resonances for a 20-cell structure (top). Under high RF power (16.5 MW peak), 24 MeV acceleration is produced in a beam with starting energy of 63.5 MeV, confirming a gradient of 91.5 MeV/m corresponding to a shunt impedance of 133 MΩ/m, comparing favorably to the simulated 155 MΩ/m (bottom). Operating at lower energy (10 MeV), much higher beam currents can be accelerated compared to conventional medical linacs to produce FLASH dose rates with 10 MV X-ray beams. (D) Cutaway view (left) and rendering of assembled (right) klystrino. This compact source (Ruler = 30 cm) operates at a modest high-voltage of 60 kV to produce 330 kW peak RF power. (E) RF phased-Array Power Distribution (RAPiD) network of waveguides (left) has 16 input ports to combine the power of 16 klystrinos (green arrows) and direct the summed power (5.3 MW peak) through appropriate phase modulation to any one of 16 output ports (red arrow) connected to 16 treatment beamlines, with a switching time of 300 ns. Thus extremely rapid electronic switching of beam directions is achieved without mechanical gantry rotation. Fabricated prototype (right) of an 8-port subunit of the RAPiD network. (F) Cutaway view (left) and assembled prototype (right) of RF pulse compressor capable of producing 6-fold pulse compression and correspondingly higher peak RF power to enable the higher accelerating gradients needed for a very-high energy electron (100 MeV) version of PHASER. (Ruler = 30.5 cm).

Typical standing-wave linacs operating at the π-mode have multiple close resonance frequencies (filling the propagation band between π-mode and the 0-mode): a structure with 20 cavities would have twenty different modes with the (π-1) being typically very close to the operating mode. As the beam loading (charge per pulse) of the structure increases, the beam becomes capable of exciting these modes and hence the beam becomes unstable. The lack of inter-cell coupling produces a single resonance frequency for the entire structure, providing much greater stability under high beam loading. A combination of high beam loading, duty factor, and the use of an array of accelerating structures simultaneously can produce the >300-fold increase in average beam current.

Prototypes of DRAGON linacs have been tested under high power at SLAC National Accelerator Laboratory, demonstrating acceleration matching simulated performance (Fig. 1A–C). Of note, the 3-D machining process to produce all of the optimized cells, RF distribution manifold, cooling channels, and other supporting features in only two parts will decrease manufacturing costs dramatically compared to the conventional cell by cell construction.

RF power sources and distribution network (RAPiD)

Fitting PHASER into existing treatment vaults requires extremely compact RF power sources that are scalable up to the needed total power, require only modest high-voltage power, and have a large duty factor. We have designed a compact klystron, a "klystrino," that generates ~330 kW of peak RF power operating at only 60 kV (Fig. 1D), allowing a compact form factor (50 cm height). The outputs of multiple klystrinos can be combined through appropriate modulation of the phases through an RF phased-Array Power Distribution (RAPiD) network [16,26] to direct the summed power to any one of multiple outputs to power an array of stationary linac beamlines with extremely rapid switching (Fig. 1E). The PHASER system will use 16 inputs (klystrinos) and 16 outputs (linacs) connected through the RAPiD network for 16-beam IMRT FLASH, in which the full complement of beams from 16 angles will be provided by the array of stationary beamlines nearly simultaneously without mechanical gantry rotation.

X-ray intensity modulation (SPHINX)

We have developed an all-electronic Scanning Pencil-beam High-speed Intensity-modulated X-ray source (SPHINX) as a replacement for MLC-based intensity modulation. Each electron beam pulse from the linac is electromagnetically steered to a specific location on an extended bremsstrahlung target (*e.g.*, a plate) to form a rapid scanning source of therapeutic energy (*e.g.*, 10 MV) X-rays, and an array of channels in a tungsten block downstream of the extended target collimates X-rays produced at each source position. Distributing the source spots on the target in space and time mitigates target heating issues [31]. The geometry of the collimator channels (illustrated schematically in Fig. 2A) is such that: (1) each spot on the source forms a pencil beamlet of X-rays the intensity of which is controlled by the intensity (number or charge

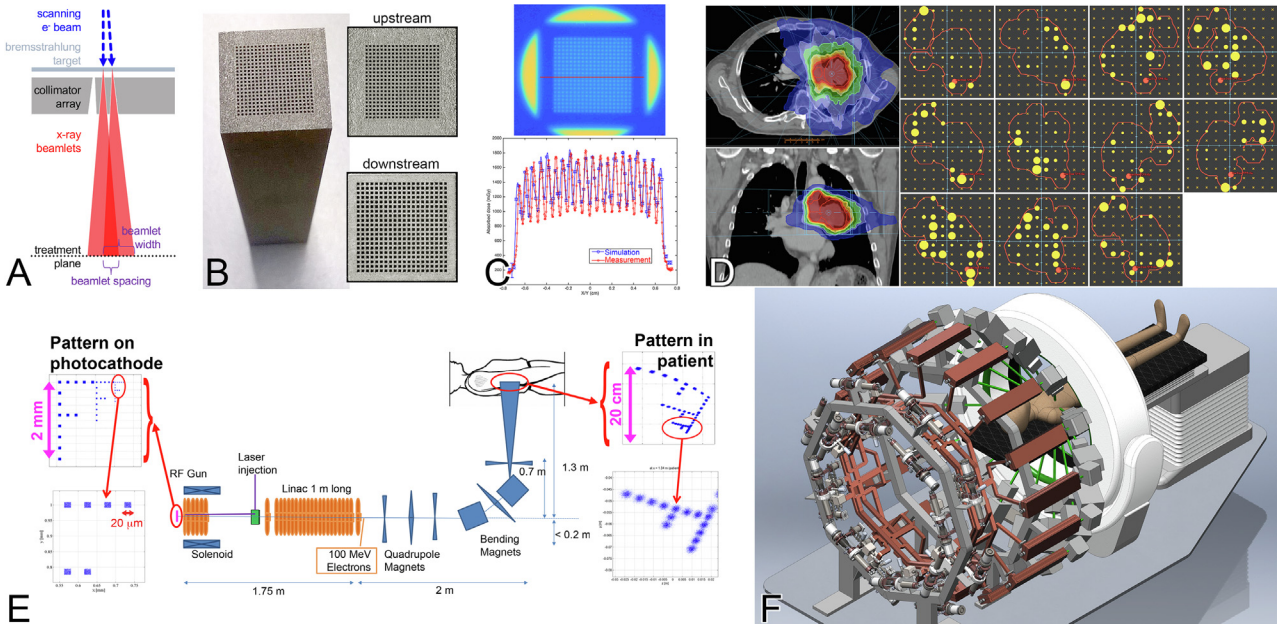

Fig. 2. (A) Schematic illustration of the Scanning Pencil-beam High-speed Intensity-modulated X-ray source (SPHINX). An electron beam is scanned on an extended bremsstrahlung target plate to produce an array of MV X-ray sources. A collimator array forms an X-ray beamlet for each source position (scale exaggerated for illustration). The channel spacing and dimensions are chosen such that the beamlet width (determined by its divergence) is larger than the inter-beamlet spacing at the treatment (isocenter) plane for coverage without dosimetric gaps and a fine selection of beamlet positions. In principle, a variety of beamlet geometries (*e.g.*, divergent, parallel, convergent) and mixture of sizes may be used. (B) A 20 × 20 channel prototype of the collimator array produced by 3-D printing of tungsten, designed to test a demanding geometry. The collimator is 10 cm thick, with channels that diverge from 300 to 400 μm width between the upstream and downstream surfaces, and whose central axes also diverge from each other. This corresponds to beamlet width of 3 mm and spacing of 1.5 mm at the isocenter plane. (C) Dimensional accuracy of the prototype was tested by placing a 6 MV X-ray source at the virtual back-focal point of the channels so that all the channels were illuminated simultaneously along their axes. Transmitted dose measured by film at the downstream surface showed good agreement with Monte-Carlo simulation. (D) Simulated SPHINX-based IMRT treatment plan for a locally advanced lung cancer. Isodose plan and beams-eye view of the 11 beam directions used in this example, depicting the inverse-optimized beamlet weights for each beamline. Total electron charge was comparable to that of the corresponding MLC-based VMAT plan. (E) Novel intensity-modulation strategy for a very high-energy electron (VHEE) version of PHASER. A spatially patterned electron source is produced by projecting an optical image onto a photocathode. The electron "image" is accelerated intact through a high-gradient DRAGON linac then steered and magnified (in a manner similar to an electron microscope) to the treatment volume in the patient, producing an intensity-modulated treatment field. Simulations demonstrate the potential of an optimized electron optics design to produce high-resolution intensity-modulation, reproducing the source intensity pattern with good fidelity. (F) Conceptual rendering of the integrated Pluridirectional High-energy Agile Scanning Electronic Radiotherapy (PHASER) system. The power of 16 klystrinos is combined through the RAPiD network and distributed to an array of 16 stationary DRAGON linacs. The non-coplanar beamlines arranged in a conical geometry share a common isocenter with a full ring multi-detector CT scanner. Each beamline includes a SPHINX system comprising scanning magnets, extended bremsstrahlung target, and collimator array to produce all-electronically intensity-modulated X-ray beams. The overall system is more compact than existing medical linacs and lacks exposed moving parts.

of pulses) of the electron beam at that spot; (2) each channel forms a diverging beamlet, but the set of beamlets can be diverging, parallel, converging, or have other nearly arbitrary geometry with respect to each other (a diverging geometry is illustrated in Fig. 2A); (3) the spacing between beamlets is fine enough to provide complete coverage of the tumor without gaps. For example, the channels can be spaced such that the divergence of the individual beamlets produces a 2:1 beamlet width to spacing ratio in the isocenter plane for fully overlapping coverage and fine choice of beamlet positioning in the treatment volume (Fig. 2A). We have manufactured a prototype with an "aggressive" geometry (3 mm beamlet width and 1.5 mm spacing at the treatment isocenter) to test the limits of our 3-D tungsten printing approach (Fig. 2B), and demonstrated by X-ray transmission measurements that high dimensional fidelity was achieved (Fig. 2C).

We simulated SPHINX-based IMRT planning by performing Monte Carlo calculation of 3-D dose from each beamlet, followed by optimization of the beamlet weights to meet planning objectives using the RayStation inverse treatment planning system (RaySearch Laboratories, Stockholm) [29,30]. For a sample case of locally advanced lung cancer, we found that a SPHINX based treatment plan demonstrated similar dose conformity and was produced using a similar total electron charge as the clinically delivered MLC-based VMAT plan (Fig. 2D).

Beamline geometry and integrated imaging

Current multi-detector CT provides high-quality volumetric imaging at sub-second speed compatible with the image-guidance requirements of PHASER [7]: for example, a typical 64-detector row scanner with 1.25 mm slice thickness at isocenter rotating at 1–2 revolutions/s (modest specifications by current standards) could acquire 2–4 imaging volumes with 50 cm radial and 8 cm longitudinal field of view each second. A non-coplanar geometry for the fixed set of beam directions allows the treatment beams and a full-ring diagnostic-quality CT imaging system to share a common isocenter for simultaneous imaging and treatment, while avoiding entrance or exit of treatment beams through radiation sensitive CT components (Fig. 2F). We evaluated treatment plans produced with beams whose central axes fall on the surface of a cone with the isocenter at the apex of the cone (conical geometry), finding favorable plan quality compared to coplanar VMAT plans for a broad range of anatomical sites [14,22,24,25]. This geometry also allows integration of a primary beam stopper ring on the opposite side of the CT scanner from the beamlines, reducing the shielding requirements of the vault.

Besides providing position verification immediately before and during rapid treatment delivery, fast diagnostic-quality CT facilitates an efficient adaptive planning work flow in which a scan at the beginning of a treatment session can be used for plan adaptation, for example by rapid selection from a set of pre-calculated plan permutations or fully re-optimizing, depending on time and computational tradeoffs [3]. In addition to much better image quality than conventional radiotherapy cone-beam CT, routine use of CT contrast is possible for optimal image-guidance in appropriately selected cases. Combining rapid imaging and delivery also creates new therapeutic possibilities such as temporally synchronizing irradiation with the intratumoral concentration peak of a bolus vascular injection of a systemic agent that can be monitored by dynamic CT imaging.

Future very high-energy electron-based PHASER

The above core PHASER technologies enabling extremely rapid delivery of MV X-ray beams ultimately serve as a platform for future developments, *e.g.*, second-generation PHASER based on very high-energy electrons (VHEE) with energies of 100–200 MeV. The concept of VHEE radiotherapy was originally proposed by DesRosiers et al. at Indiana University [4,18], although practical technologies to realize it were unavailable at that time. Advantages of VHEE include depth-dose and scattering characteristics enabling favorable dose conformity and integral dose intermediate between photons and protons, insensitivity to tissue density heterogeneity, and compatibility with rapid electronic beam delivery [1,2,17,21].

PHASER technology can be used to produce VHEE beams in a straightforward way by applying higher peak RF power to generate higher accelerating gradients in DRAGON linacs using a larger number of klystrinos. Since much lower beam current is needed when treating directly with VHEE without bremsstrahlung conversion, pulse length can be traded for higher peak power through pulse compression [27,8]. We have developed a highly compact, low-cost pulse compression system to produce a 6-fold higher peak power for correspondingly higher accelerating gradient (Fig. 1F).

While intensity-modulation can be achieved by raster scanning an electron pencil beam from each beamline, we propose a more robust solution as follows. Rather than a point-like electron source, a spatially patterned (*i.e.*, intensity-modulated) electron source can be produced by projecting an optical pattern or "image" onto a photocathode (such as with a scanning laser or a variety of spatial light modulators). A corresponding electron "image" is then emitted from the photocathode and is accelerated through a linac to the full beam energy with its spatial structure preserved. In a manner analogous to an electron microscope, the electron image is then steered and magnified using magnetic electron optics with high fidelity to the treatment target in the patient. The entire intensity-modulated field from each beam direction (beamline) is delivered at once without the need for raster scanning. Simulations demonstrate the potential of an optimized electron optics design to produce high-resolution intensity-modulation (Fig. 2E).

Conclusion

FLASH irradiation can be performed preclinically in small volume and/or superficial targets using electrons, synchrotron X-rays, and protons [23,10,15,19,13]. However, to translate FLASH to general deep-seated radiotherapy targets in humans requires accelerator performance hundreds of times greater than existing technologies.

PHASER comprises several core innovations to enable near instantaneous delivery of highly conformal image-guided radiotherapy that will eliminate the impact of tumor motion and potentially exploit a superior FLASH radiobiological therapeutic index. Compactness, power efficiency, and economical manufacturing are key design considerations (Supplemental Fig.). The lack of moving mechanical parts contributes to serviceability and removes patient collision as a safety consideration. Diagnostic quality CT image-guidance facilitates adaptive planning and is well suited to its automation through machine learning approaches, leading to high clinical efficiency and throughput. If these factors are fully realized, PHASER will improve clinical outcomes, cost effectiveness, and accessibility of cancer care worldwide [20].

Sources of support

This work was supported by the Stanford University Department of Radiation Oncology, the Weston Havens Foundation, the Stanford University School of Medicine, the Stanford University Office of the Provost, the SLAC National Accelerator Laboratory, the U.S. Department of Energy, the Wallace H. Coulter Foundation,

the Swedish Childhood Cancer Foundation, Sweden, the Foundation BLANCEFLOR Boncompagni Ludovisi n'ee Bildt, Sweden, the American Association for Cancer Research, the Stanford Bio-X Interdisciplinary Initiatives Program, the Stanford Cancer Imaging Training Program, the U.S. Department of Defense Lung Cancer Research Program, the National Cancer Institute (1R43CA217607-01), the Australian National Health and Medical Research Council, the American Association of Physicists in Medicine, the Cancer League, the Li Ka Shing Foundation, and RaySearch Laboratories, Sweden.

Acknowledgements

The authors are deeply indebted to many individuals for their crucial scientific contributions and valuable discussions, in particular: Magdalena Bazalova-Carter, Vinod Bharadwaj, Philipp Borchard, Karl Bush, Justin Carter, Erica Cherry Kemmerling, Eric Colby, Valery Dolgashev, Michael Dunning, Neville Eclov, Kjell Eriksson, Rebecca Fahrig, Andrew Haase, Björn Hårdemark, Carsten Hast, Erik Hemsing, Elin Hynning, David Jaffray, Christopher Jensen, Keith Jobe, Anna Kim, Gregory King, Ryan Ko, Albert Koong, Quynh-Thu Le, Zenghai Li, Cecile Limborg, Michael Liu, Doug McCormick, Timothy Mitchell, Christopher Nantista, Janice Nelson, Ludovic Nicolas, Karl Otto, Bianey Palma, Bradley Qu, Emil Schüler, Aaron Tremaine, Stefania Trovati, Jinghui Wang, Juwen Wang, Lei Wang, Minna Wedenberg, Dian Yeremian.

Disclosures

BWL, PGM, and SGT are co-inventors on Stanford patents pertaining to PHASER related technologies. BWL, PGM, and SGT are co-founders of TibaRay. BWL and SGT are board members of TibaRay.

Appendix

Here we provide a more detailed explanation of radiofrequency (RF) power efficiency as it applies to our DRAGON linac design. The literature has multiple definitions for the so-called shunt impedance, a parameter related to how much RF power is required to establish the accelerating gradient in the linac structure and goes toward producing waste heat. Some definitions do not include the transit-time factor, and some apply only to a single cell within the structure rather than the whole structure [11]. Within the community of medical linac designers, the shunt impedance is typically quoted for a single cell, and sometimes the quote includes the product of the shunt impedance and the transit-time factor.

The convention we follow in this article uses a definition adopted by high energy physics linac designers, which is:

$$R_s \equiv \frac{G^2}{\partial p/\partial z}$$

where R_s is the shunt impedance, G is the local accelerating gradient (the total acceleration seen by the particle including transit-time factor), and $\partial p/\partial z$ is the rate of power loss along the length of the structure [32]. For our case of equally distributed power along the structure this quantity becomes:

$$R_s = \frac{V^2}{LP}$$

where V is the total accelerating potential (voltage) to which the electrons are accelerated, L is the length of the accelerator structure, and P is the RF power feeding the structure.

From the published data for typical medical linacs [11], the best (highest) shunt impedance for a single cell is ~100 MΩ/m. However, from the same published data one can estimate the overall shunt impedance for the whole structure by knowing the beam current, energy, the total input RF power, and the structure length. Using our definition of shunt impedance, this comes closer to 50 MΩ/m for current state-of-the-art medical linacs, compared to the 130–200 MΩ/m in our DRAGON structures.

Given our definition of shunt impedance, the peak (within a pulse) power consumed by the structure to establish the accelerating gradient (which ends up as waste heat) [32] is:

$$P_s = \frac{V^2}{LR_s}$$

whereas the peak power consumed by accelerating the beam ("useful" power) is:

$$P_b = VI_{peak}$$

where I_{peak} is the current of the accelerated electron pulse. Hence, the RF-to-beam efficiency (proportion of applied RF power that goes into the accelerated electron beam) is given by:

$$\eta_{RF-to-beam} = \frac{VI_{peak}}{VI_{peak} + \frac{V^2}{LR_s}} = \frac{1}{1 + \frac{V}{I_{peak}LR_s}}$$

Thus the efficiency of the DRAGON structure is greatly enhanced by its stability under high beam loading (charge per pulse and therefore beam current) and high shunt impedance. For example, a DRAGON structure operating at 11.4 GHz and optimized for 10 MeV/m gradient has a shunt impedance of 200 MΩ/m, such that a meter-long structure producing a 10 MeV beam at 300 mA peak current would have a RF-to-beam-efficiency of about 86%. Including losses in the initial few cells that provide beam bunching and low energy acceleration, the overall RF-to-beam efficiency could be expected to be around 80%, compared to about 18% (at S-band) to up to 45% (at X-band) in current state-of-the-art medical linacs.

Appendix A. Supplementary data

Supplementary data to this article can be found online at https://doi.org/10.1016/j.radonc.2019.05.005.

References

[1] Bazalova-Carter M, Liu M, Palma B, et al. Comparison of film measurements and Monte Carlo simulations of dose delivered with very high-energy electron beams in a polystyrene phantom. Med Phys 2015;42(4):1606–13.
[2] Bazalova-Carter M, Qu B, Palma B, et al. Treatment planning for radiotherapy with very high-energy electron beams and comparison of VHEE and VMAT plans. Med Phys 2015;42(5):2615–25.
[3] Cherry Kemmerling EM, Wu M, Yang H, Maxim PG, Loo Jr BW, Fahrig R. Optimization of an on-board imaging system for extremely rapid radiation therapy. Med Phys 2015;42(11):6757–67.
[4] DesRosiers C, Moskvin V, Bielajew AF, Papiez L. 150–250 meV electron beams in radiation therapy. Phys Med Biol 2000;45(7):1781–805.
[5] Dolgashev V, Tantawi S, Higashi Y, Spataro B. Geometric dependence of radio-frequency breakdown in normal conducting accelerating structures. Appl Phys Lett 2010;97(17):171501-1 to -3.
[6] Favaudon V, Caplier L, Monceau V, et al. Ultrahigh dose-rate FLASH irradiation increases the differential response between normal and tumor tissue in mice. Sci Transl Med 2014;6(245):245ra93.
[7] Flohr TG, Schaller S, Stierstorfer K, Bruder H, Ohnesorge BM, Schoepf UJ. Multi–detector row CT systems and image-reconstruction techniques. Radiology 2005;235(3):756–73.
[8] Franzi M, Wang JW, Dolgashev V, Tantawi S. Compact rf polarizer and its application to pulse compression systems. Phys Rev Accel Beams 2016;19(6):062002–1 to -10.
[9] Grudiev A, Calatroni S, Wuensch W. New local field quantity describing the high gradient limit of accelerating structures. Phys Rev Spec Top-Accel Beams 2009;12(10):102001-1 to -9.
[10] Jaccard M, Duran MT, Petersson K, et al. High dose-per-pulse electron beam dosimetry: Commissioning of the Oriatron eRT6 prototype linear accelerator for preclinical use. Med Phys 2018;45(2):863–74.

[11] Karzmark CJ, Nunan CS, Tanabe E. Medical electron accelerators. New York: McGraw-Hill; 1993.
[12] Laurent L, Tantawi S, Dolgashev V, et al. Experimental study of rf pulsed heating. Phys Rev Spec Top-Accel Beams 2011;14:041001–1 to -21.
[13] Lempart M, Blad B, Adrian G, et al. Modifying a clinical linear accelerator for delivery of ultra-high dose rate irradiation. Radiother Oncol 2019;139:40–5.
[14] Mitchell T, Maxim P, Hadsell M, Loo Jr BW. Investigating the dose distributions of equiangular spaced noncoplanar beams. Med Phys 2015;42(6):3453.
[15] Montay-Gruel P, Bouchet A, Jaccard M, et al. X-rays can trigger the FLASH effect: Ultra-high dose-rate synchrotron light source prevents normal brain injury after whole brain irradiation in mice. Radiother Oncol 2018;129 (3):582–8.
[16] Nantista CD, Tantawi SG. A compact, planar, eight-port waveguide power divider/combiner: The cross potent superhybrid. IEEE Microw Guided Wave Lett 2000;10(12):520–2.
[17] Palma B, Bazalova-Carter M, Hårdemark B, et al. Assessment of the quality of very high-energy electron radiotherapy planning. Radiother Oncol 2016;119 (1):154–8.
[18] Papiez L. Very high energy electromagnetically-scanned electron beams are an attractive alternative to photon IMRT. For the proposition. *Med Phys* 2004;31 (7):1945–6.
[19] Patriarca A, Fouillade C, Auger M, et al. Experimental set-up for FLASH proton irradiation of small animals using a clinical system. Int J Radiat Oncol Biol Phys 2018;102(3):619–26.
[20] Pistenmaa D, Dosanjh M, Amaldi U, et al. Changing the global radiation therapy paradigm. Radiother Oncol 2018;128(3):393–9.
[21] Schüler E, Eriksson K, Hynning E, et al. Very high-energy electron (VHEE) beams in radiation therapy; treatment plan comparison between VHEE, VMAT, and PPBS. Med Phys 2017;44(6):2544–55.
[22] Schüler E, Loo Jr BW, Maxim P. Conical beam geometry in radiation therapy. Med Phys 2017;44(6):3209.
[23] Schüler E, Trovati S, King G, et al. Experimental platform for ultra-high dose rate FLASH irradiation of small animals using a clinical linear accelerator. Int J Radiat Oncol Biol Phys 2017;97(1):195–203.
[24] Schüler E, Wang L, Loo Jr BW, Maxim P. Feasibility of a novel conical beams arrangement in radiation therapy. Med Phys 2018;45(6):E127.
[25] Schüler E, Wang L, Loo Jr BW, Maxim PG. Conical beam geometry intensity-modulated radiation therapy. Phys Med Biol 2019. In press.
[26] Tantawi SG, Nantista C, Kroll N, et al. Multimoded rf delay line distribution system for the Next Linear Collider. Phys Rev Spec Top-Accel Beams 2002;5 (3):032001–1 to -8.
[27] Tantawi SG, Nantista CD, Dolgashev VA, et al. High-power multimode X-band RF pulse compression system for future linear colliders. Phys Rev Spec Top-Accel Beams 2005;8(4). pp. 042002–1 to -19.
[28] Tantawi SG, Nasr M, Li Z, Limborg CG, Borchard P. Distributed coupling accelerator structures: a new paradigm for high gradient linacs. arXiv:181109925 2018.
[29] Trovati S, Borchard P, King GJ, et al. Validation of a novel therapeutic X-ray array source and collimation system. Med Phys 2016;43(6):3767–8.
[30] Trovati S, Schueler E, King G, Hynning E, Loo B, Maxim P. A method for the generation of treatment plans for a novel X-ray target and collimation system (SPHINX). Med Phys 2017;44(6):1.
[31] Wang J, Trovati S, Borchard PM, Loo Jr BW, Maxim PG, Fahrig R. Thermal limits on MV X-ray production by bremsstrahlung targets in the context of novel linear accelerators. Med Phys 2017;44(12):6610–20.
[32] Wang JW. RF properties of periodic accelerating structures for linear colliders. SLAC Report Number 339 1989.